

# Construction of a dispersion relation from an arbitrary density of states

MARCUS KOLLAR

*Institut für Theoretische Physik,  
Johann Wolfgang Goethe-Universität Frankfurt,  
Robert-Mayer-Straße 8-10, D-60054 Frankfurt am Main, Germany*

The dispersion relations of energy bands in solids are characterized by their density of states, but a given density of states may originate from various band structures. We show how a spherically symmetric dispersion can be constructed for any one-band density of states. This method is applied to one-, two- and three-dimensional systems. It also serves to establish that any one-band spectrum with finite bandwidth can be obtained from a properly scaled dispersion relation in the limit of infinite dimensions.

*Keywords:* Electronic band structure, dynamical mean-field theory, nesting symmetry

## 1. Introduction

The band structure of electrons describes their quantum-mechanical motion in the periodic potential of a crystal lattice in the absence of interactions. This picture is modified by the Coulomb interaction between them, which must be taken into account accurately to understand the phenomena observed in strongly correlated systems such as transition-metal oxides, ferromagnetic metals, or the cuprate superconductors. Nonetheless the properties of the non-interacting lattice system remain an important input quantity.

The electronic spectrum of a solid is characterized by the density of states,

$$N(\omega) = \frac{1}{V_B} \int dk_1 \cdots \int dk_D \delta(\omega - \epsilon_{\vec{k}}), \quad (1)$$

where the integral is over the first Brillouin zone, which has volume  $V_B$ ; here and in the following we consider only a single separated band  $\epsilon_{\vec{k}}$ . The mapping from dispersion relation to density of states is not invertible, i.e., two different dispersions may lead to the same function  $N(\omega)$ . Nevertheless in certain situations it is desirable to construct a dispersion that corresponds to a particular  $N(\omega)$ . In this paper we present a method that performs this inversion in any dimension  $D$ , with additional assumptions on the functional form of  $\epsilon_{\vec{k}}$ .

Construction of a dispersion with given spectral properties is especially of interest within the framework of dynamical mean-field theory (DMFT) for Hubbard-type models, which becomes exact in the limit of infinite dimensions,  $D \rightarrow \infty$ .<sup>1,2</sup> In this

approach typical tight-binding dispersions, arising from hopping of electrons between orbitals on neighboring lattice sites, lead to a density of states which extends to infinite values of  $\omega$ . For example, on the hypercubic lattice  $N(\omega)$  becomes a Gaussian bell curve<sup>1</sup>

$$N(\omega) = \frac{1}{\sqrt{2\pi}} \exp\left(-\frac{\omega^2}{2}\right). \quad (2)$$

Exponential tails are also obtained for the generalized face-centered cubic lattice<sup>3</sup> and the generalized diamond lattice.<sup>4</sup>

The DMFT is particularly well suited to describe the Mott-Hubbard metal-insulator transition.<sup>5</sup> In order to work with a finite bandwidth, which better models finite-dimensional systems, DMFT studies of this transition (for recent work see Ref. 6 and references therein) have concentrated on next-neighbor hopping on the Bethe lattice in the limit of infinite connectivity. It leads to a semi-circular density of states,<sup>2</sup>

$$N(\omega) = \frac{2}{\pi} \sqrt{1 - \omega^2}, \quad |\omega| \leq 1, \quad (3)$$

which in this case is defined via the one-particle Green's function, since there is no underlying periodic crystal lattice and hence no dispersion relation. The Bethe lattice has hitherto been the only known infinite-dimensional system with a finite bandwidth. Below we will show how a dispersion can be constructed on a  $D$ -dimensional crystal lattice that in the limit  $D \rightarrow \infty$  yields any given density of states with finite bandwidth, providing an answer to one of the open conceptual questions about this limit.

In DMFT all one-particle quantities in the homogeneous phase involve the dispersion only implicitly through  $N(\omega)$ . Therefore another standard approach has been to use a function  $N(\omega)$  that derives from a dispersion on a finite-dimensional lattice or is tuned by hand. For instance, Wahle *et al.*<sup>7</sup> introduced the model density of states,

$$N(\omega) = \frac{1 + \sqrt{1 - a^2}}{\pi} \frac{\sqrt{1 - \omega^2}}{1 + a\omega}, \quad |\omega| \leq 1, \quad (4)$$

to study the effect of asymmetry in  $N(\omega)$  on the stability of ferromagnetism in the Hubbard model. Here  $a \in [-1; 1]$  is a tunable parameter; (4) reduces to the symmetric function (3) for  $a = 0$ . For  $a > 0$  spectral weight is shifted towards the lower band edge, while for  $a = 1$   $N(\omega)$  has a square-root singularity at  $\omega = -1$  similar to the tight-binding density of states for the fcc lattice. Below we will derive dispersions in  $D = 1, 2, 3, \infty$  that represent this density of states.

## 2. Isotropic Fermi surfaces on Bravais lattices

We construct a dispersion with a given density of states as follows. In terms of the latter the band filling  $n(\mu)$  for Fermi energy  $\mu$  is given by

$$n(\mu) = \int_{\omega_{\min}}^{\mu} d\omega N(\omega), \quad (5)$$

which lies between 0 and 1. Suppose now that the dispersion relation is spherically symmetric,  $\epsilon_{\vec{k}} = \epsilon(|\vec{k}|)$ , with  $|\vec{k}|^2 = k_1^2 + \dots + k_D^2$ . Furthermore we assume that  $\epsilon(k)$  increases with  $k$ ; then the Fermi sea is simply connected and includes the point  $\vec{k} = 0$ , and there is a one-to-one relation between Fermi energy  $\mu$  and Fermi vector  $k$ . The band filling can thus be obtained in another, geometric way as the normalized volume of the Fermi sea,  $v_D(k)$ , defined by

$$v_D(k) = \int_0^k dk' s_D(k'), \quad (6)$$

where  $s_D(k)$  is its normalized surface,

$$s_D(k) = \frac{1}{V_B} \int dk_1 \dots \int dk_D \delta\left(k - \sqrt{k_1^2 + \dots + k_D^2}\right). \quad (7)$$

The dispersion  $\epsilon(k)$  is now defined by setting  $v_D(k)$  equal to the band filling calculated from the density of states, i.e.,

$$v_D(k) = n(\epsilon(k)). \quad (8)$$

As is appropriate for a one-band density of states we assume  $N(\omega) > 0$  for  $\omega_{\min} < \omega < \omega_{\max}$ , so that  $n(\mu)$  is invertible on this interval. In terms of its inverse function  $\mu(n)$  we can write

$$\epsilon(k) = \mu(v_D(k)). \quad (9)$$

Note that the functional form of  $\mu(n)$  depends only on the given density of states  $N(\omega)$ , whereas that of  $v_D(k)$  depends only on the crystal lattice. Once the latter has been calculated for a lattice of interest,  $\epsilon(k)$  is immediately available for any  $N(\omega)$ .

Similarly, the density of states can be at once calculated from a given spherically symmetric dispersion  $\epsilon(k)$ , provided  $\epsilon'(k) > 0$ . In terms of  $k(\epsilon)$ , the inverse function of  $\epsilon(k)$ , we have  $n(\epsilon) = v_D(k(\epsilon))$  from (9), and hence

$$N(\epsilon) = n'(\epsilon) = s_D(k(\epsilon)) k'(\epsilon). \quad (10)$$

To apply the method in either direction it remains to calculate the functions  $s_D(k)$  and  $v_D(k)$ .

### 3. Dimensions $D = 1, 2, 3$

We consider now the special case of a hypercubic lattice in  $D$  dimensions, treating explicitly the cases  $D = 1, 2, 3$ , as well as the limit  $D \rightarrow \infty$ . For convenience we measure  $k$  in units of  $2\pi/a$ , where  $a$  is the lattice spacing, so that the first Brillouin zone is located in the region  $|k_i| < \frac{1}{2}$ , and the maximum value for  $|\vec{k}|$  is  $\sqrt{D}/2$ . For  $k \leq \frac{1}{2}$  the integrations in (7) can be performed in spherical coordinates, since the vector  $\vec{k}$  always remains within the first Brillouin zone. In this case we have  $s_D(k) = S_D k^{D-1}$  and  $v_D(k) = V_D k^D$ , where  $S_D = 2\pi^{D/2}/\Gamma(D/2)$  and  $V_D = \pi^{D/2}/\Gamma(1 + D/2)$  are the surface and volume of the  $D$ -dimensional unit sphere, respectively. This case applies for all  $k$  in  $D = 1$ , so that

$$s_1(k) = 2, \quad v_1(k) = 2k, \quad \text{for } k \in [0; \frac{1}{2}], \quad (11)$$

representing the contribution of the two Fermi points. The spherical symmetry reduces to inversion symmetry in this simple case, which was discussed already in Ref. 7.

For the square lattice in  $D = 2$  the values  $0 \leq k \leq \sqrt{2}/2$  are allowed. However if  $k > \frac{1}{2}$  only that part of a circle with radius  $k$  contributes which lies inside the square Brillouin zone, as shown in the inset of Figure 1. We obtain

$$s_2(k) = \begin{cases} 2\pi k & \text{if } k \in [0; \frac{1}{2}] \\ 2\pi k - 8k \arccos \frac{1}{2k} & \text{if } k \in [\frac{1}{2}; \frac{\sqrt{2}}{2}] \end{cases}, \quad (12)$$

and by integrating with respect to  $k$ ,

$$v_2(k) = \begin{cases} \pi k^2 & \text{if } k \in [0; \frac{1}{2}] \\ \pi k^2 + \sqrt{4k^2 - 1} - 4k^2 \arccos \frac{1}{2k} & \text{if } k \in [\frac{1}{2}; \frac{\sqrt{2}}{2}] \end{cases}. \quad (13)$$

These functions are shown in Figure 1.

In  $D = 3$  the Brillouin zone of the simple cubic lattice allows the values  $0 \leq k \leq \sqrt{3}/2$ , and more cases must be distinguished in the calculation of  $s_3(k)$ . We omit geometric considerations and instead employ the recursion formula for  $s_D(k)$  on the hypercubic lattice,

$$s_{D+1}(k) = \int_{\max(0, k^2 - \frac{1}{4})^{\frac{1}{2}}}^{\min(k, \frac{\sqrt{D}}{2})} dq \frac{2k s_D(q)}{\sqrt{k^2 - q^2}}, \quad (14)$$

which can be obtained in a straightforward fashion from (7). Applying it to the above expression for  $s_2(k)$  we obtain, after a lengthy calculation,

$$s_3(k) = \begin{cases} 4\pi k^2 & \text{if } k \in [0; \frac{1}{2}] \\ 6\pi k - 8\pi k^2 & \text{if } k \in [\frac{1}{2}; \frac{\sqrt{2}}{2}] \\ 6\pi k - 8\pi k^2 + 48k^2 \arctan \sqrt{1 - \frac{1}{2k^2}} & \text{if } k \in [\frac{\sqrt{2}}{2}; \frac{\sqrt{3}}{2}] \\ -24k \arctan \sqrt{4k^2 - 2} & \text{if } k \in [\frac{\sqrt{2}}{2}; \frac{\sqrt{3}}{2}] \end{cases}, \quad (15)$$

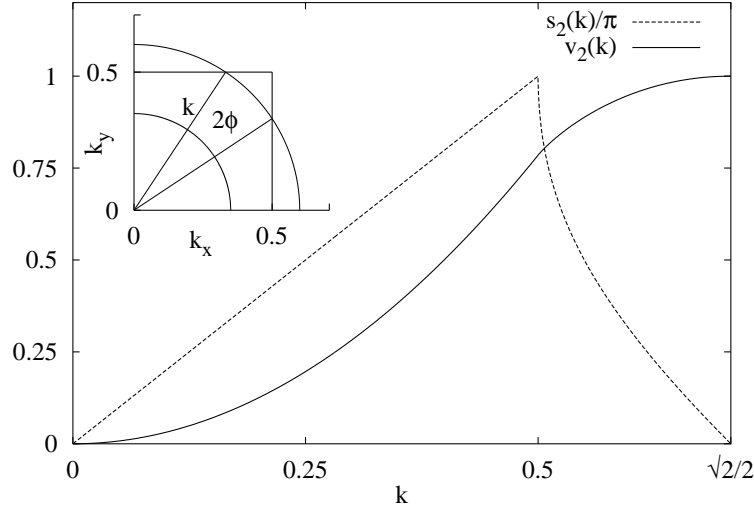


Fig. 1. Surface  $s_2(k)$  and volume  $v_2(k)$  of a circular Fermi sea with Fermi vector  $k$  on the square lattice. Inset: If the Fermi surface has radius  $k \leq \frac{1}{2}$  it lies completely within the first Brillouin zone. If  $k > \frac{1}{2}$  the inside part contributes  $2\phi k$  in each quadrant to  $s_2(k)$ , where  $\cos \phi = 1/(2k)$ , leading to (12).

and one more integration yields

$$v_3(k) = \begin{cases} \frac{4}{3}\pi k^3 & \text{if } k \in [0; \frac{1}{2}] \\ 3\pi k^2 - \frac{8}{3}\pi k^3 - \frac{\pi}{4} & \text{if } k \in [\frac{1}{2}; \frac{\sqrt{2}}{2}] \\ 3\pi k^2 - \frac{8}{3}\pi k^3 - \frac{\pi}{4} + 16k^3 \arctan \sqrt{1 - \frac{1}{2k^2}} \\ + \sqrt{4k^2 - 2} - (12k^2 - 1) \arctan \sqrt{4k^2 - 2} & \text{if } k \in [\frac{\sqrt{2}}{2}; \frac{\sqrt{3}}{2}] \end{cases} \quad (16)$$

These functions are displayed in Figure 2.

As a simple example, let us consider the rectangular (constant) density of states

$$N(\omega) = 1, \quad 0 \leq \omega \leq 1, \quad (17)$$

where  $\mu(n) = n$ , and hence  $\epsilon(k) = v_D(k)$ . Thus the plot of  $v_D(k)$  in Figures 1 and 2 also represents the shape of the dispersion that will yield the density of states (17). Next we apply the method to the model density of states (4). The band filling is now obtained as

$$n(\mu) = 1 - \frac{1 + \sqrt{1 - a^2}}{\pi a^2} \left( \arccos \mu - a \sqrt{1 - \mu^2} - 2\sqrt{1 - a^2} \arctan \left[ \frac{(1 - a)(1 - \mu)}{(1 + a)(1 + \mu)} \right]^{\frac{1}{2}} \right), \quad (18)$$

which for the Bethe lattice ( $a = 0$ ) reduces to  $n(\mu) = \frac{1}{2} + [\mu\sqrt{1 - \mu^2} + \arcsin \mu]/\pi$ . The resulting dispersion relations are shown in Figure 3. Their curvature depends

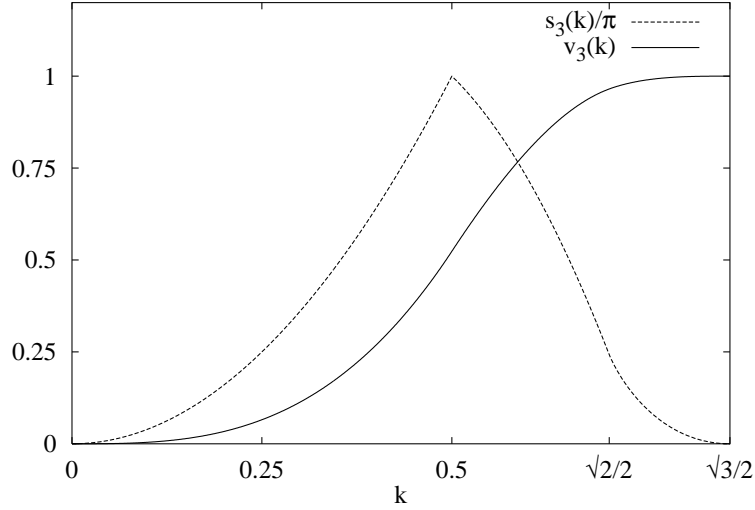


Fig. 2. Surface  $s_3(k)$  and volume  $v_3(k)$  of a spherical Fermi sea with Fermi vector  $k$  on the simple cubic lattice.

strongly on the asymmetry parameter  $a$ , and also on  $D$ .

Another quantity of interest is the hopping amplitude between two lattice sites connected by a lattice vector  $\vec{R} = (R_1, \dots, R_D)$  with integer components. It is defined as (note the conventional overall minus sign)

$$t(\vec{R}) = - \int_{-\frac{1}{2}}^{\frac{1}{2}} dk_1 \cdots \int_{-\frac{1}{2}}^{\frac{1}{2}} dk_D \epsilon(\sqrt{k_1^2 + \cdots + k_D^2}) e^{2\pi i \vec{k} \cdot \vec{R}}. \quad (19)$$

We calculate the hopping amplitude (19) for the one-dimensional dispersion (Figure 3a). For small  $R$  we find that the amplitudes for hopping between nearest and between next-nearest neighbors,  $t(1)$  and  $t(2)$ , are of opposite sign, and  $|t(2)/t(1)|$  is appreciable for  $a$  close to 1; for example  $t(1) = 0.337$ ,  $t(2) = -0.080$ , for  $a = 0.95$ . For large  $|R|$  it can be shown<sup>8</sup> that  $t(R) \propto (-1)^R |R|^{-5/3}$ . While the stabilization of the ferromagnetic phase was attributed to large spectral weight below the Fermi energy in Ref. 7, the present calculation shows that from a complementary point of view (4) can be regarded approximately as a  $t$ - $t'$  model, which has been shown to be favorable for ferromagnetism by other methods.<sup>9</sup>

#### 4. Limit of large dimensions

Finally we turn to the limit  $D \rightarrow \infty$ . To obtain a factorized expression for  $s_D(k)$  for the hypercubic lattice we transform the argument of the delta function and use

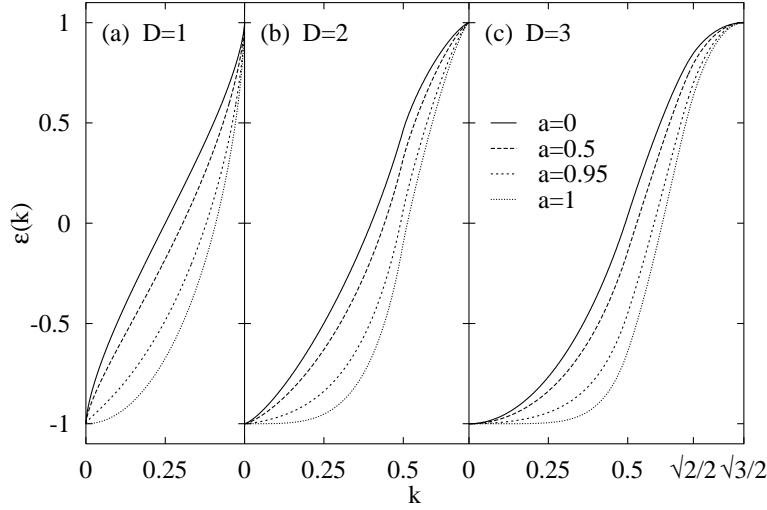


Fig. 3. Dispersions in  $D = 1, 2, 3$  leading to the model density of states (4) for several values of the asymmetry parameter  $a$ .

the representation  $\delta(x) = \int_{-\infty}^{\infty} dt e^{itx} / (2\pi)$ ,

$$s_D(k) = 2k \int_{-\frac{1}{2}}^{\frac{1}{2}} dk_1 \cdots \int_{-\frac{1}{2}}^{\frac{1}{2}} dk_D \delta(k_1^2 + \cdots + k_D^2 - k^2), \quad (20)$$

$$= \frac{k}{\pi} \int_{-\infty}^{\infty} dt e^{-itk^2} g_0(t)^D, \quad (21)$$

where we defined  $g_0(t) = \int_{-1/2}^{1/2} dq e^{itq^2}$ . The maximum value for  $k$  is  $\sqrt{D}/2$ ; it is useful to introduce scaled quantities,  $\kappa = 2k/\sqrt{D}$  and  $\bar{s}_D(\kappa) = s_D(\kappa\sqrt{D}/2)\sqrt{D}/2$ ,  $\bar{v}_D(\kappa) = v_D(\kappa\sqrt{D}/2)$ , with the property  $\int_0^1 d\kappa \bar{s}_D(\kappa) = \bar{v}_D(1) = 1$ . We change variables to  $s = tD/4$ ,

$$\bar{s}_D(\kappa) = \frac{\kappa}{\pi} \int_{-\infty}^{\infty} ds e^{-is\kappa^2} g_0\left(\frac{4s}{D}\right)^D. \quad (22)$$

This equation is valid for all  $D$ . From the expansion  $g_0(t) = 1 + it/12 - t^2/160 + O(t^3)$  we obtain for large  $D$

$$g_0\left(\frac{4s}{D}\right)^D = \exp\left(\frac{is}{3} - \frac{s^2}{10D}\right) (1 + O(\frac{1}{D^2})), \quad (23)$$

which, when substituted into (22), leads to a sharply peaked Gaussian for large  $D$ ,

$$\bar{s}_D(\kappa) = \frac{2\kappa}{\sqrt{2\pi}\sigma} \exp\left(-\frac{(\kappa^2 - \frac{1}{3})^2}{2\sigma^2}\right) (1 + O(\frac{1}{D^2})), \quad (24)$$

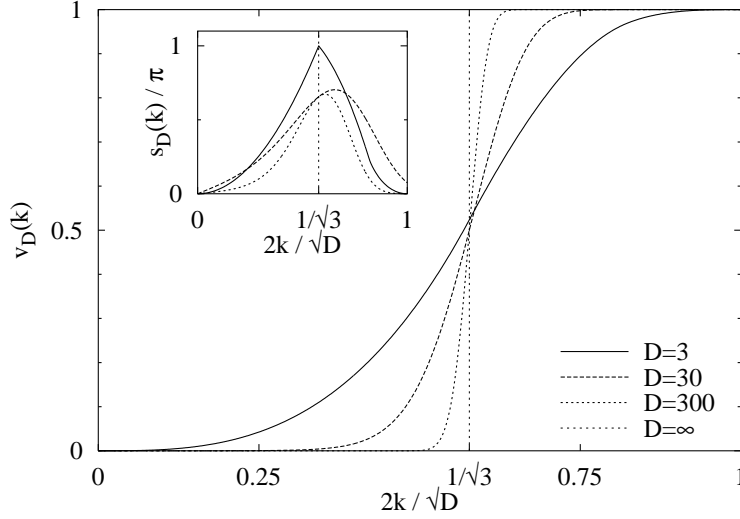


Fig. 4. Weight functions  $s_D(k)$  and  $v_D(k)$ , approaching (24) and (25) for large dimensions  $D$ . For  $D = 3$  the closed forms (15) and (16) are shown. For example, in dimension  $D$  the dispersion  $\epsilon(k) = v_D(k)$  will yield the rectangular density of states (17).

with the abbreviation  $\sigma = 1/\sqrt{5D}$ . We find that for large  $D$  the function  $\bar{s}_D(\kappa)$  eventually approaches a delta function,  $\bar{s}_D(\kappa) \sim \delta(\kappa - 1/\sqrt{3})$  and  $s_D(k) \sim \delta(k - \sqrt{D/12})$ . This surprisingly simple result means that in this limit the Fermi sea is essentially located in a narrow hyperspherical shell (cut off at the Brillouin zone boundaries) at roughly half the maximum value of  $k$ . Interestingly, the Fermi surface has the same average radius as for the tight-binding dispersion with nearest-neighbor hopping.<sup>10</sup> The Fermi surface in the latter case is distributed with a Gaussian in  $\kappa - 1/\sqrt{3}$  instead of  $\kappa^2 - 1/3$ ; these distributions become equivalent for  $D \rightarrow \infty$ .

Next we obtain the asymptotic expression for  $\bar{v}_D(\kappa)$  from (24) to the same order,

$$\bar{v}_D(\kappa) = \begin{cases} \frac{1}{2} \left[ \operatorname{erfc}\left(\frac{1-3\kappa^2}{3\sqrt{2}\sigma}\right) - \operatorname{erfc}\left(\frac{1}{3\sqrt{2}\sigma}\right) \right] & \text{if } \kappa \in [0; \frac{1}{\sqrt{3}}] \\ 1 - \frac{1}{2} \left[ \operatorname{erfc}\left(\frac{3\kappa^2-1}{3\sqrt{2}\sigma}\right) + \operatorname{erfc}\left(\frac{1}{3\sqrt{2}\sigma}\right) \right] & \text{if } \kappa \in [\frac{1}{\sqrt{3}}; 1] \end{cases}. \quad (25)$$

This function ultimately approaches a step function,  $\bar{v}_D(\kappa) \sim \Theta(\kappa - 1/\sqrt{3})$  and  $v_D(k) \sim \Theta(k - \sqrt{D/12})$ ; however further calculations must be performed with the asymptotic expressions (24) and (25) instead of the delta and step functions. In particular (9) and (25) prescribe how to construct a dispersion that in the limit of infinite dimensions will yield any desired  $N(\omega)$  with finite bandwidth, for example (3) or (4). The functions  $\bar{v}_D(\kappa)$  and  $\bar{s}_D(\kappa)$  are shown in Figure 4. As  $D$  approaches infinity, the dispersion thus has the form of a smoothed-out step function, changed in shape by the application of  $\mu(n)$ .

Let us consider some examples. As noted above the plot of  $v_D(k)$  in Figure 4 already shows the dispersion that yields the rectangular density of states (17). On



the other hand, for the special quadratic dispersion

$$\epsilon(k) = \sqrt{5D} \left( \frac{4k^2}{D} - \frac{1}{3} \right), \quad (26)$$

we use (24) and (10) to obtain the corresponding density of states

$$N(\omega) = \frac{1}{\sqrt{2\pi}} \exp\left(-\frac{\omega^2}{2}\right), \quad -\sqrt{5D}/3 \leq \omega \leq 2\sqrt{5D}/3, \quad (27)$$

to leading order in  $1/D$ . Hence in the limit  $D \rightarrow \infty$  the dispersion (26) yields the Gaussian (2). This shows that the tight-binding spectrum for next-neighbor hopping on the hypercubic lattice may alternatively be represented by a quadratic dispersion in the limit  $D \rightarrow \infty$ .

It is instructive to calculate the hopping amplitude (19) corresponding to the dispersion (9) in the limit of large  $D$ . We change variables to  $|\vec{k}|$ , introduce the scaled dispersion  $\bar{\epsilon}(\kappa) = \epsilon(\kappa\sqrt{D}/2)$ , and perform a similar factorization as before, with the result (valid for all  $D$ )

$$t(\vec{R}) = - \int_0^1 d\kappa \frac{\kappa \bar{\epsilon}(\kappa)}{\pi} \int_{-\infty}^{\infty} ds e^{-is\kappa^2} \prod_{j=1}^D g_{R_j}(\frac{4s}{D})^D, \quad (28)$$

where we introduced  $g_R(t) = \int_{-1/2}^{1/2} dq e^{itq^2 + 2\pi i q R}$ . Note that by setting  $\vec{R} = 0$  in (28) the center of mass of the band,  $t(0) = \int_{\omega_{\min}}^{\omega_{\max}} d\omega \omega N(\omega)$ , is correctly recovered. Proceeding to the limit  $D \rightarrow \infty$  we first observe that  $g_R(t) = -it(-1)^R/(2\pi^2 R^2) + O(t^2)$  for integer  $R \neq 0$ . The hopping amplitude along a coordinate axis is then calculated to leading order in  $1/D$  as

$$\begin{aligned} t_1(R_1) &\equiv t((R_1, 0, \dots, 0)) \\ &= \frac{(-1)^{R_1}}{D\pi^2 R_1^2} \int_0^1 d\kappa \frac{\kappa \bar{\epsilon}(\kappa)}{\pi} \int_{-\infty}^{\infty} ds 2is \exp\left[is\left(\frac{1}{3} - \kappa^2\right) - \frac{s^2}{10D}\right] \\ &= \frac{(-1)^{R_1}}{D\pi^2 R_1^2} \int_0^1 d\kappa \bar{\epsilon}(\kappa) \frac{d}{d\kappa} \left( -\frac{\bar{s}_D(\kappa)}{\kappa} \right). \end{aligned} \quad (29)$$

Using (24) the remaining integral is calculated by partial integration and yields  $\sqrt{3} \bar{\epsilon}'(1/\sqrt{3})$ , which is evaluated via (9),

$$\bar{\epsilon}'(\kappa) = \mu'(\bar{v}_D(\kappa)) \bar{s}_D(\kappa) = \frac{\bar{s}_D(\kappa)}{N(\mu(\bar{v}_D(\kappa)))}. \quad (30)$$

To leading order in  $1/D$  we have  $\bar{s}_D(1/\sqrt{3}) = \sqrt{10D/3\pi}$  and  $\bar{v}_D(1/\sqrt{3}) = \frac{1}{2}$ , whence

$$t_1(R_1) = \frac{t_1^*}{\sqrt{D}} \frac{(-1)^{R_1}}{R_1^2}, \quad t_1^* = \frac{\sqrt{10}}{\pi^{\frac{5}{2}} N(\mu(\frac{1}{2}))}. \quad (31)$$

The numerical factor  $t_1^*$  contains the value of the density of states at the Fermi energy for a half-filled band,  $\mu(\frac{1}{2})$ . For fixed  $R_1$  this type of hopping takes place from

each site to  $2D$  other lattice sites, and the hopping amplitude is scaled proportional to the inverse square root of this coordination number, which is also the required scaling for a tight-binding band with hopping to nearest neighbors.<sup>1</sup> An important difference is that in the present case the hopping is long ranged and slowly decaying. It is also apparent that  $t(\vec{R})$  has higher symmetry than the crystal lattice, which is a consequence of the spherical symmetry of  $\epsilon_{\vec{k}}$ . This spherical symmetry is also responsible for the large amplitude for long-range hopping, as any type of finite-range hopping would lead to a dispersion relation with only a discrete symmetry.

In similar fashion we calculate the hopping amplitude between two sites connected by a lattice vector with two nonzero entries,  $t_2(R_1, R_2) \equiv t((R_1, R_2, 0, \dots, 0))$ ,

$$t_2(R_1, R_2) = \frac{t_2^*}{D} \frac{(-1)^{R_1+R_2}}{R_1^2 R_2^2}, \quad t_2^* = \frac{10N'(\mu(\frac{1}{2}))}{\pi^5 N(\mu(\frac{1}{2}))^3}. \quad (32)$$

The value of  $t_2^*$  now also involves the first derivative of the density of states; for example,  $t_2^* = -0.080$  and  $t_1^* = 0.839$  for (4) with  $a = 0.95$ , but  $t_2^* = 0$  for (3). The number of sites connected by hopping of type (32) is proportional to  $D^2$ , the square root of which again appears in the scaling factor as expected. We conclude that although each hopping amplitude is scaled with dimension in the same way as in the tight-binding case, the present long-range hopping amplitudes combine to yield an energy band with a finite width, in contrast to the infinite tails in the tight-binding spectrum.

Finally, note that the nesting symmetry,  $\epsilon_{\vec{k}} = -\epsilon_{\vec{k}+\vec{Q}}$ , which results if hopping takes place only between different sublattices of a bipartite lattice, is absent for a spherically symmetric dispersion. Here  $\vec{k} + \vec{Q}$  is taken modulo the first Brillouin zone and the antiferromagnetic wave vector is  $\vec{Q} = (\frac{1}{2}, \frac{1}{2}, \dots, \frac{1}{2})$  in our notation. For example, the spherically symmetric representation (26) of the Gaussian density of states yields

$$\epsilon_{\vec{k}+\vec{Q}} = \sqrt{5D} \left( \frac{4k^2}{D} + \frac{2}{3} - \frac{4}{D} \sum_{i=1}^D |k_i| \right) \quad (33)$$

for  $|k_i| \leq \frac{1}{2}$ . Hence  $\epsilon_{\vec{k}} \neq -\epsilon_{\vec{k}+\vec{Q}}$  for most of the Brillouin zone, in particular on or near the Fermi surface, where  $|k_i| = \frac{1}{2\sqrt{3}} + O(D^{-1/2})$ . That the nesting condition is not fulfilled can also be seen from the fact that sites on the same sublattice are connected by the long-range hopping amplitude (31). In general, this frustration is expected to suppress antiferromagnetism in the Hubbard model, which is of interest in particular for the study of the Mott-Hubbard metal-insulator transition in the paramagnetic phase. It seems that spherically symmetric dispersion relations offer a conceptually and computationally simpler way to remove the antiferromagnetic phase than, e.g., “fully frustrated” hopping on the Bethe lattice.<sup>2</sup>

## 5. Conclusion and outlook

In conclusion we presented a method that, for any crystal lattice, maps a one-band density of states to a dispersion  $\epsilon_{\vec{k}}$  that only depends on  $|\vec{k}|$ . This procedure unphysically enlarges the usual invariance of the dispersion under the point group of the crystal to a continuous spherical symmetry. As a consequence, the nesting symmetry typical for nearest-neighbor hopping on bipartite lattices is absent. Furthermore, the dispersion may have kinks if the specified density of states has van Hove singularities that are inappropriate for the dimension  $D$  of the representing lattice. On the other hand, the spherical symmetry may allow for analytic calculations of DMFT one-particle quantities in the homogeneous phase that depend on the dispersion only through the density of states, such as the Green function of the Hubbard model in the vicinity of the Mott-Hubbard metal-insulator transition.

## Acknowledgements

The author would like to thank S. Sachdev and D. Vollhardt for valuable discussions. During a stay at Yale University this research was supported by US NSF Grant DMR 0098226.

## References

1. W. Metzner and D. Vollhardt, *Phys. Rev. Lett.* **62**, 324 (1989).
2. A. Georges, G. Kotliar, W. Krauth, and M. Rozenberg, *Rev. Mod. Phys.* **68**, 13 (1996).
3. E. Müller-Hartmann, *Proceedings of the V. Symposium "Physics of Metals,"* eds. E. Talik and J. Szade (Ustroń, Poland, 1991), p. 22.
4. G. Santoro, M. Airoldi, S. Sorella, and E. Tosatti, *Phys. Rev. Lett.* **47**, 16216 (1993).
5. F. Gebhard, *The Mott Metal-Insulator Transition* (Springer, Berlin, 1997).
6. R. Bulla, T. A. Costi, and D. Vollhardt, *Phys. Rev.* **B64**, 045103 (2001).
7. J. Wahle, N. Blümer, J. Schlipf, K. Held, and D. Vollhardt, *Phys. Rev.* **B58**, 12749 (1998).
8. P. G. J. van Dongen, private communication.
9. S. Daul and R. M. Noack, *Phys. Rev.* **B58**, 2635 (1998).
10. E. Müller-Hartmann, *Z. Phys.* **B76**, 211 (1989).